Journal of Power Sources 183 (2008) 418–421

Contents lists available at ScienceDirect

Journal of Power Sources

journal homepage: www.elsevier.com/locate/jpowsour

Short communication

Mechanochemical synthesis of α-Fe_2O_3 nanoparticles and their application to all-solid-state lithium batteries☆

Hirokazu Kitaura, Kenji Takahashi, Fuminori Mizuno, Akitoshi Hayashi, Kiyoharu Tadanaga, Masahiro Tatsumisago*

Department of Applied Chemistry, Graduate School of Engineering, Osaka Prefecture University, 1-1 Gakuen-cho, Nakaku, Sakai, Osaka 599-8531, Japan

ARTICLE INFO

Article history:
Available online 18 May 2008

Keywords:
Lithium
Fe_2O_3
All-solid-state
Batteries
Mechanochemical
Nanoparticles

ABSTRACT

α-Fe_2O_3 fine particles have been prepared by a mechanochemical process and a solution process. α-Fe_2O_3 nanoparticles with aggregates composed of the several tens nm primary particles were produced by the mechanochemical process. The nanoparticles were applied to the electrode as an active material for all-solid-state lithium batteries and the electrochemical properties of the cell were investigated. Typical charge–discharge curves, as seen in the liquid type cell using the α-Fe_2O_3 nanoparticles as an electrode were observed in the all-solid-state cell. The first discharge capacity of the cell of about 780 mAh g^{-1} was, however, smaller than the capacity of a cell using α-Fe_2O_3 particles prepared by the solution process, which were monodispersed particles of 250 nm without aggregates. In order to develop electrochemical performance of all-solid-state batteries, it is important to use the electrode particles without aggregation which lead to the formation of good solid–solid interface between active material and solid electrolyte particles.C

1. Introduction

Rechargeable lithium ion batteries with high energy density have been widely used as power sources for various portable equipments. In general, volatile and flammable organic liquid electrolytes are used for commercially available batteries and then the demand of the safer lithium ion batteries increases. The use of the nonflammable solid electrolytes instead of liquid electrolytes is pointed out as an effective way to produce the lithium ion batteries with high safety and high reliability. We prepared sulfide glass-based solid electrolytes and found that Li_2S–P_2S_5-based glass–ceramics exhibited high ambient temperature conductivities of about 10^{-3} S cm^{-1} [1,2]. We then assembled all-solid-state rechargeable batteries using these glass–ceramics as a solid electrolyte [3–5]. The all-solid-state In/$LiCoO_2$ cells showed an excellent cycle performance with a constant discharge capacity of over 100 mAh g^{-1} and coulomb efficiencies of 100% for 500 cycles [6].

We have investigated negative electrode materials that can be used for all-solid-state lithium batteries with the highly conductive solid electrolytes [7,8]. Recently, 3*d*-transition metal oxides are studied as negative electrode materials for lithium batteries [9]. In particular, iron oxides are promising materials from the viewpoint of economic and environmental aspect. We have just reported that the various sizes of α-Fe_2O_3 highly dispersive particles were prepared by a solution process called "gel–sol" technique, which was reported by Sugimoto et al. [10], and were applied to the active materials for all-solid-state lithium batteries [11]. The all-solid-state cells of Li–In/Li_2S–P_2S_5 glass–ceramics/α-Fe_2O_3 worked as lithium rechargeable battery and showed the similar charge–discharge reaction mechanism to that of the cell with liquid electrolytes. The first discharge capacities of the cells with several sizes of α-Fe_2O_3 increased with decreasing the size of the active materials [11]. However, it was difficult to prepare particles of less than 100 nm by the gel–sol technique.

Nanoparticles are generally defined as the particles of less than 100 nm in diameter. In particular, as the size of nanoparticles is less than several tens nm, the ultrafine particles exhibit the different properties from those of the bulk materials and are attracting much attention in a variety of fields. McCormick et al. synthesized a series of nanocrystalline materials by a mechanochemical process [12–14]. α-Fe_2O_3 nanoparticles were also synthesized by the mechanochemical process. The mechanical milling of the mixture of $FeCl_3$ and CaO (or $Ca(OH)_2$) using a mixer mill apparatus produced the composite of α-Fe_2O_3 and $CaCl_2$, and the separated α-Fe_2O_3 nanoparticles of 20–50 nm were obtained by the removal of the $CaCl_2$. In this method, $CaCl_2$ works as a matrix to suppress the grain growth of α-Fe_2O_3.

☆ Presented at the IMLB 2006-International Meeting on Lithium Batteries.

* Corresponding author.
E-mail address: tatsu@chem.osakafu-u.ac.jp (M. Tatsumisago).

0378-7753/$ – see front matter © 2008 Elsevier B.V. All rights reserved.
doi:10.1016/j.jpowsour.2008.05.032

In this paper, the synthesis of α-Fe_2O_3 nanoparticles by mechanical milling of the mixture of $FeCl_3$ and Na_2CO_3 using a planetary ball mill apparatus is reported. All-solid-state cells were assembled with the prepared α-Fe_2O_3 nanoparticles as an electrode. In the cells, the Li_2S–P_2S_5-based glass–ceramic was used as a solid electrolyte. Their electrochemical properties were compared to those of the cells with α-Fe_2O_3 particles prepared by the gel–sol technique. The influences of the morphology and size of α-Fe_2O_3 particles on the performance of all-solid-state cells will be discussed.

2. Experimental

α-Fe_2O_3 particles were prepared by the mechanochemical method. $FeCl_3$ (95%, Wako Pure Chemical) and Na_2CO_3 (99.5%, Wako Pure Chemical) as starting materials were weighted and mixed in an agate mortar. The molar ratio of $[FeCl_3]/[Na_2CO_3] = 2/3$ was selected. The mixture was then put into a 45 ml stainless-steel pot together with 10 zirconia balls of 10 mm in diameter. The pot was sealed and set in a planetary ball mill apparatus (Fritsch, Pulverisette 7). Mechanical milling treatment was carried out at a rotating speed of 510 rpm for 20 h. The mechanochemically milled powder was washed by deionized water using an ultrasonic bath and a centrifuge. The obtained powder was dried *in vacuo*.

The α-Fe_2O_3 particles, the size of which size is 250 nm, were prepared by a solution process and the detailed experimental procedure is reported previously [10]. 5.4 M NaOH aqueous solution was added to 2.0 M $FeCl_3$ aqueous solution and then the mixed solution was aged for 8 days at 100 °C in an oven. The precipitation in the solution was dried after washing and the α-Fe_2O_3 particles were obtained.

X-ray diffraction (XRD) measurement (Cu Kα) was performed using a diffractometer (MAC Science, M18XHF^{22}-SRA) to identify crystalline phases and determine crystallite size. Two main peaks at around 33° and 35° in 2θ of the patterns were chosen for the calculation of crystallite size by use of the Scherrer's equation.

Specific surface area was determined using the Brunauer–Emmett–Teller (BET) method and pore volume was calculated by the Barrett–Joyner–Halenda (BJH) method with a surface area measuring instrument (Micrometritics, Tristar 3000). Before this analysis, the samples were preheated for 3 h at 130 °C *in vacuo*.

The microstructure and morphology of the samples were examined by using a field emission scanning electron microscope (Hitachi, FE-SEM, S-4500).

All-solid-state electrochemical cells were assembled as follows [3]. The $80Li_2S{\cdot}20P_2S_5$ (mol%) glass was prepared by the mechanical milling process and then the glass–ceramic electrolyte was prepared by crystallizing the glass at around 230 °C [1,3]. The obtained glass–ceramic with high conductivity of 10^{-3} S cm^{-1} (at 25 °C) was used as a solid electrolyte for all-solid-state cells. A composite electrode as a working electrode was prepared by mixing of α-Fe_2O_3 (37.7 wt.%), the solid electrolyte (56.6 wt.%), and acetylene-black (5.7 wt.%) powders. The composite electrode (10 mg) and solid electrolyte powder (80 mg) were set in a polycarbonate tube and then were pressed under 3700 kg cm^{-2}. Li–In alloy, which was formed by attaching an indium foil of 300 μm in thickness and lithium foil of 250 μm in thickness, as a counter and reference electrode, respectively, was put on the solid electrolyte layer, and the three-layered pellet was sandwiched by two stainless-steel disks as current collectors. Two electrode cells were obtained after pressing under 1200 kg cm^{-2}. Galvanostatic tests of the cells were conducted under current density of 64 μA cm^{-2} at 25 °C in an Ar atmosphere using a charge–discharge measuring device (Nagano Co., BTS-2004).

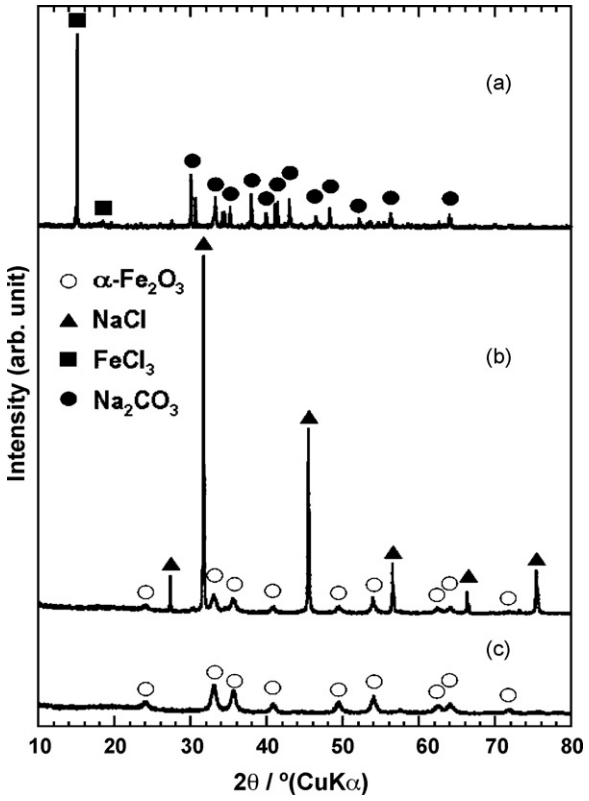

Fig. 1. XRD patterns of (a) as-mixed powder, (b) milled powder and (c) washed powder with deionized water after milling.

3. Results and discussion

Fig. 1 shows XRD patterns of (a) as-mixed and (b) milled powders. The XRD pattern of (c) washed powder after milled for 20 h is also shown. The patterns of the starting materials are observed in the as-mixed powder. The peaks of the powder milled for 20 h are attributable to those of α-Fe_2O_3 and NaCl crystals. It indicates that the reaction proceeded by mechanical milling for 20 h as follows:

$$2FeCl_3 + 3Na_2CO_3 \rightarrow Fe_2O_3 + 6NaCl + 3CO_2$$

The XRD pattern of washed powder shows the peaks corresponding to only α-Fe_2O_3. It is found that the NaCl phase was completely removed by washing and then only α-Fe_2O_3 powders are obtained.

Fig. 2 shows the SEM image of the particles of α-Fe_2O_3 prepared by the mechanochemical process. The α-Fe_2O_3 was composed of aggregates with primary particles of several tens nm, suggesting that α-Fe_2O_3 nanoparticles were successfully obtained by the mechanochemical process. In this process, the composite of α-Fe_2O_3 and NaCl was produced as the result of the reaction of $FeCl_3$ and Na_2CO_3. It is expected that NaCl particles work as the matrix, which prevents α-Fe_2O_3 particles from growing, and then α-Fe_2O_3 nanoparticles are obtained. The SEM image of the particles of α-Fe_2O_3 prepared by the solution process called "gel–sol" technique is also shown in Fig. 2. The size of highly dispersive particles is about 250 nm and the size distribution is small. Table 1 lists the particle size from the SEM image, crystallite size from the XRD measurement, BET specific surface area and pore volume of the particles prepared by the mechanochemical process and the solution process. The crystallite size of α-Fe_2O_3 prepared by the mechanochemical process is about 14 nm, which is smaller than that of α-Fe_2O_3 prepared by the solution process. The BET specific

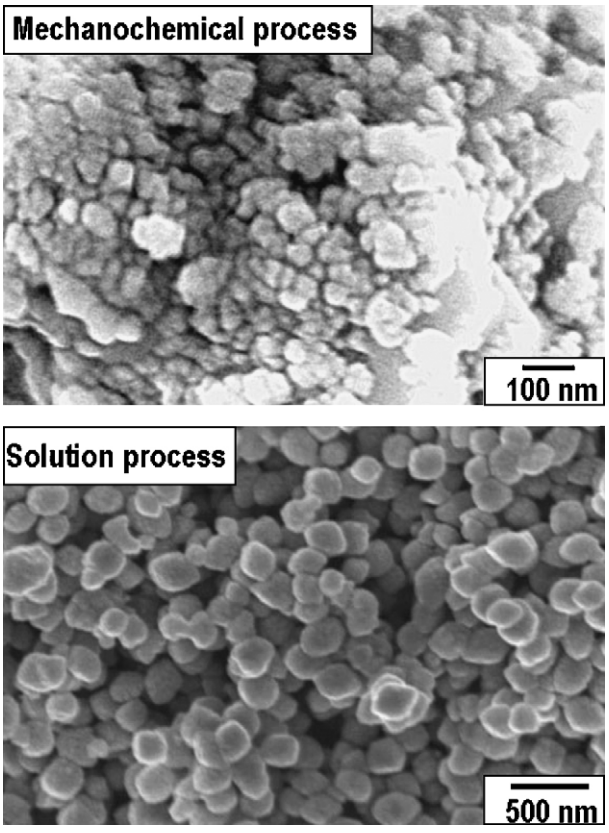

Fig. 2. SEM images of α-Fe_2O_3 particles prepared by a mechanochemical process and a solution process.

surface area and the pore volume of the mechanochemically prepared α-Fe_2O_3 are respectively 46 $m^2\,g^{-1}$ and 0.15 $cm^3\,g^{-1}$, which are larger than those of α-Fe_2O_3 prepared by the solution process.

Fig. 3 shows the first charge and discharge curves of all-solid-state cells Li–In/α-Fe_2O_3 prepared by the mechanochemical process. The measurements were performed between fixed voltage limits of 0.6 and 2.6 V (versus Li). In this figure, the axis of ordinate on the left side denotes the cell potential versus Li–In counter electrode, and that on the right side denotes the potential versus the Li electrode, which was calculated from the basis of potential difference between Li–In and Li [15]. The α-Fe_2O_3 particle prepared by the mechanochemical process works as the active material of the all-solid-state cells and the first discharge capacity is about 780 mAh g^{-1}. The first charge and discharge curves of α-Fe_2O_3 particles with about 250 nm in diameter as shown in Fig. 2 prepared by the solution process are also shown in Fig. 3. The first discharge capacity is about 1050 mAh g^{-1} and is larger than that of α-Fe_2O_3 prepared by the mechanochemical process. The difference of the capacity would be due to the degree of aggregation of the α-Fe_2O_3 particles. Active materials which electrically connect with the solid electrolytes only work in the all-solid-state

Table 1
Particle size averaged from the SEM image, crystallite size calculated using Scherrer's equation, BET specific surface area and BJH pore volume of the α-Fe_2O_3 particles prepared by a mechanochemical process and a solution process

Sample	Particle size (nm)	Crystallite size (nm)	BET surface area ($m^2\,g^{-1}$)	Pore volume ($cm^3\,g^{-1}$)
Mechanochemical process	Several tens	14	46	0.15
Solution process	250	50	20	0.09

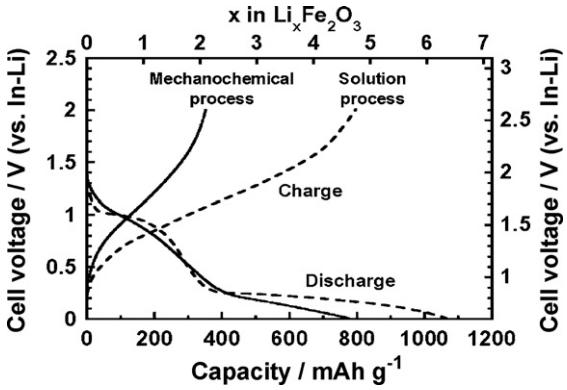

Fig. 3. First charge–discharge curves of all-solid-state cells with α-Fe_2O_3 prepared by a mechanochemical process and a solution process as an active material. The cells were discharged and charged between 0.6 and 2.6 V (versus Li).

batteries. α-Fe_2O_3 particles prepared by the mechanochemical process formed the aggregates; the active materials at the center of aggregates, which have no contact with the solid electrolyte, are electrochemically inactive and the utilization of the active materials is not enough. On the other hand, α-Fe_2O_3 particles prepared by the solution process were larger than the particles prepared by the mechanochemical process but formed no aggregates. However, such active materials have a good contact with the solid electrolytes and show larger capacity. It is necessary to prepare nanoparticles without aggregation for the purpose of increasing the specific capacity. It has been reported that the α-Fe_2O_3 particles with smaller crystallites less than 20 nm and higher specific surface area were prepared [16–18]. The utilization of dispersive nanoparticles would be effective to develop all-solid-state lithium batteries.

The first discharge curve in the α-Fe_2O_3 prepared by the mechanochemical process shows two slopes from around 1.6 and 0.8 V (versus Li), while the curve in the α-Fe_2O_3 prepared by the solution process shows two plateaus at around 1.6 and 0.8 V (versus Li). In our previous study of XRD measurements of the electrode using α-Fe_2O_3 particles prepared by the solution process at various levels of discharge and charge, we have examined the charge–discharge reaction mechanism in the all-solid-state cells. It was revealed that the plateau at around 1.6 V corresponds to a lithium insertion process into the structure of α-Fe_2O_3, and the plateau at around 0.8 V corresponds to the formation process of Fe and Li_2O phases [11]. In the conventional cells with a liquid electrolyte, the reaction mechanism of reactivity of α-Fe_2O_3 has been evaluated in detail using XRD, X-ray absorption fine structure, and Mössbauer [16–18]. The reaction mechanism of the solid-state cell is basically similar to that of the corresponding liquid electrolyte cell. The plateau at around 1.6 V was observed in the cases using α-Fe_2O_3 particles with small crystallite size, and large pore volume [11]. The slope from around 1.6 V in the α-Fe_2O_3 prepared by the mechanochemical process would correspond to the lithium insertion process because of the α-Fe_2O_3 particles have a small crystallite size and relatively large pore volume as shown in Table 1. The slope from 0.8 V would corresponds to the formation process of Fe and Li_2O phases.

Fig. 4 shows the charge–discharge capacities and charge–discharge efficiencies of the all-solid-state cell of Li–In/α-Fe_2O_3 prepared by the mechanochemical process as a function of cycle number. Solid and open circles denote charge and discharge capacities, respectively, and solid squares denote charge–discharge efficiencies. The capacities gradually decrease with increasing the cycle number, and the cell shows the capacity of about 130 mAh g^{-1}

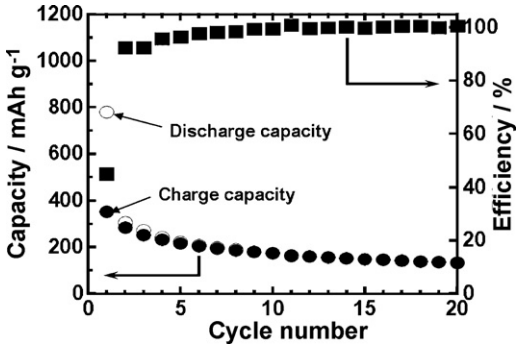

Fig. 4. Cycle performance of the all-solid-state cell with α-Fe_2O_3 prepared by a mechanochemical process with the cut-off voltage of 0.6 and 2.6 V (versus Li).

at the 20th cycle. The capacity fading was also observed in the all-solid-state cells using α-Fe_2O_3 prepared by the solution process [11]. In our previous study, ex situ XRD measurements of the electrodes after cycling were performed to investigate the reaction mechanism and the cause of the capacity loss. The mechanism of electrochemical reaction of α-Fe_2O_3 and lithium in the all-solid-state cells was determined as follows:

$$\alpha\text{-}Fe_2O_3 \rightarrow Li_xFe_2O_3 \rightarrow \text{cubic } Li_2Fe_2O_3 \Leftrightarrow Fe + \text{amorphous } Li_2O$$

In the discharge process, lithium ion is inserted into the hexagonal structure of α-Fe_2O_3, and then the hexagonal phase transforms into cubic phase. Further lithiation leads to the formation of metallic Fe and amorphous Li_2O. In the charge process, the formation reaction of Fe and Li_2O is reversible and cubic $Li_2Fe_2O_3$ is formed. The peaks of Fe were, however, observed in XRD pattern of the electrode after the 20th charging, suggesting that a large Fe domain, which is electrochemically inactive, partially formed on the discharge process. The capacity loss of the cell using mechanochemically prepared α-Fe_2O_3 as shown in Fig. 4 would also be caused by the formation of such inactive Fe domains during cycling.

4. Conclusion

α-Fe_2O_3 nanoparticles were prepared by the mechanochemical process. The particles were composed of aggregates with primary particles of several tens nm. All-solid-state cells of Li–In alloy/Li_2S–P_2S_5 glass–ceramics/α-Fe_2O_3 worked as rechargeable lithium batteries and showed initial discharge capacity of about 780 mAh g^{-1}. The capacity was smaller than that of the cell with α-Fe_2O_3 particles prepared by the solution process (diameter with about 250 nm). The reversible capacity decreased during cycling and reached about 130 mAh g^{-1} after 20 cycles. Preventing the aggregation of electrode nanoparticles would be effective to improve specific capacity of all-solid-state cells.

Acknowledgements

This work was supported by Industrial Technology Research Grant Program from New Energy and Industrial Technology Development Organization (NEDO) of Japan.

References

[1] A. Hayashi, S. Hama, H. Morimoto, M. Tatsumisago, T. Minami, Chem. Lett. (2001) 872.
[2] F. Mizuno, A. Hayashi, K. Tadanaga, M. Tatsumisago, Adv. Mater. 17 (2005) 918.
[3] F. Mizuno, S. Hama, A. Hayashi, K. Tadanaga, T. Minami, M. Tatsumisago, Chem. Lett. (2002) 1244.
[4] A. Hayashi, S. Hama, F. Mizuno, K. Tadanaga, T. Minami, M. Tatsumisago, Solid State Ionics 175 (2004) 683.
[5] T. Minami (Ed.), Solid State Ionics for Batteries, Springer-Verlag, Tokyo, 2005, p. 53.
[6] M. Tatsumisago, F. Mizuno, A. Hayashi, J. Power Sources 159 (2006) 193.
[7] A. Hayashi, T. Konishi, K. Tadanaga, T. Minami, M. Tatsumisago, J. Power Sources 146 (2005) 496.
[8] A. Hayashi, T. Konishi, K. Tadanaga, M. Tatsumisago, Solid State Ionics 177 (2006) 2737.
[9] P. Poizot, S. Laruelle, S. Grugeon, L. Dupont, J.M. Tarascon, Nature 407 (2000) 496.
[10] T. Sugimoto, K. Sakata, A. Muramatsu, J. Colloid Interface Sci. 159 (1993) 372.
[11] H. Kitaura, K. Takahashi, F. Mizuno, A. Hayashi, K. Tadanaga, M. Tatsumisago, J. Electrochem. Soc. 154 (2007) A725.
[12] J. Ding, W.F. Miao, P.G. McCormick, R. Street, Appl. Phys. Lett. 67 (1995) 3804.
[13] T. Tsuzuki, P.G. McCormick, J. Mater. Sci. 39 (2004) 5143.
[14] J. Ding, T. Tsuzuki, P.G. McCormick, Nanostruct. Mater. 8 (1997) 739.
[15] K. Takada, N. Aotani, K. Iwamoto, S. Kondo, Solid State Ionics 86–88 (1996) 877.
[16] D. Larcher, C. Masquelier, D. Bonnin, Y. Chabre, V. Masson, J.B. Leriche, J.M. Tarascon, J. Electrochem. Soc. 150 (2003) A133.
[17] D. Larcher, D. Bonnin, R. Cortes, I. Rivals, L. Personnaz, J.M. Tarascon, J. Electrochem. Soc. 150 (2003) A1643.
[18] G. Jain, M. Balasubramanian, J.J. Xu, Chem. Mater. 18 (2006) 423.